Computers and Geotechnics **15** (1993) 221–245

FINITE ELEMENT ANALYSES OF BRIDGE ABUTMENTS ON FIRM CLAY

M D Bolton

Cambridge University Engineering Department
Trumpington Street, Cambridge
England. CB2 1PZ

H W SUN

WS Atkins Consultants Ltd, Geotechnical Division
Woodcote Grove, Ashley Road, Epsom
Surrey, England. KT18 5BW

and

A M Britto

Transport and Road Research Laboratory
Old Wokingham Road, Crowthorne
Berkshire, England. RG11 6AU

ABSTRACT

In finite element analysis of soil-structure interaction problems involving firm to stiff overconsolidated clay, there have been difficulties in modelling the stress-strain response of the soil. Non-linearity and anisotropy of the soil depend on the inherent anisotropy of its particle structure and the induced anisotropy of its stress history and current stress path.

In CRISP modelling of the centrifuge test of an abutment wall and its backfill of sand on the surface of a firm to stiff overconsolidated kaolin, the clay foundation was divided into 6 broad zones in accordance with the stress history and stress path. Undrained movements of the abutment and its subsoil were closely modelled in two analyses; one with a non-linear elastic model and the other with the Schofield model with shear modulus G assigned to the foundation zone in accordance with the estimated strain level as well as stress history and stress path.

In the prediction of consolidation movement, there is a difficulty in the current critical state soil model in CRISP. The fe solution incorrectly predicted that substantial horizontal movement would accompany settlement due to consolidation, whereas the centrifuge test showed mainly vertical movement. This is attributable to the pronounced anisotropy separately observed in element tests.

INTRODUCTION

Movement of an abutment wall, due to the construction of the backfill and the embankment construction behind, is important in bridge design. A recent study by the FHWA, US Department of Transportation [1] on the performance of bridge abutments shows that lateral movement at the bridge deck level is critical to the serviceability of the bridge structure. For example, if the abutment moves too far towards the deck, it will jam, causing a thrust in the bridge deck which it will not have been designed to carry. Economic design may be achieved from better understanding of the soil-structure interaction of the spread base abutment wall on clay (figure 1). This paper will describe the finite element analysis of the movement of the abutment wall and its clay foundation, comparing with the results from a series of centrifuge model tests.

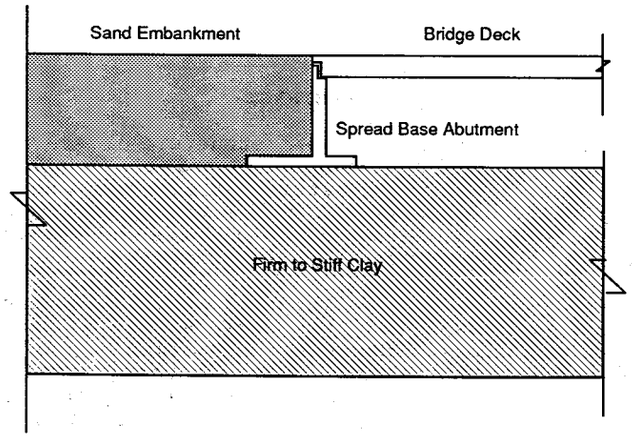

FIGURE 1. Full-height spread base bridge abutment

THE CENTRIFUGE MODELS

Centrifuge model testing is useful in the investigation of geotechnical problems where idealized conditions may be created to

allow the validation of analytical or numerical solutions. Figure 2 shows a typical 1/100 centrifuge model (test HWS7) from this series of experiments which examine the behaviour of abutment walls free standing on firm clay. The kaolin clay foundation was initially consolidated to a maximum vertical pressure of 660kPa in a consolidometer, and then allowed to swell back to a vertical pressure of 66kPa before the clay was removed from the consolidometer and trimmed to the dimensions of the model. The clay model was then placed in the strongbox, and the front surface was marked with a matrix of black plastic bullets, which were used to measure subsoil displacements from photographs taken through the Perspex window in-flight. The aluminium alloy model wall, which modelled the bending stiffness of a 1-m thick reinforced concrete prototype, was instrumented with 13 bending moment transducers. Seven displacement transducers were used to monitor the displacement of the wall and one to measure ground settlement in front of the wall base.

After the clay foundation reached pore pressure equilibrium by continuous swelling near the top and re-compression near the bottom, the lateral effective stresses could be inferred from the known cycles of vertical effective stress, through the 1-D data of consolidation and swelling obtained by Al-Tabbaa [2]. These states of stress are shown in figure 3.

Shear vane tests were conducted at different depths in the clay foundation to measure the consistency of the model. Figure 4 shows the undrained shear strength profile measured by in-flight shear vane tests. Then, a sand embankment was placed in-flight by pouring sand from a hopper located above the model. Embankment construction caused an immediate heave, forward translation and backward rotation of the wall reference axes.

Figure 5 shows the displacements of the clay foundation just after the embankment construction was completed in test HWS3, revealed by measuring the in-flight photographs before and after sand-pouring.

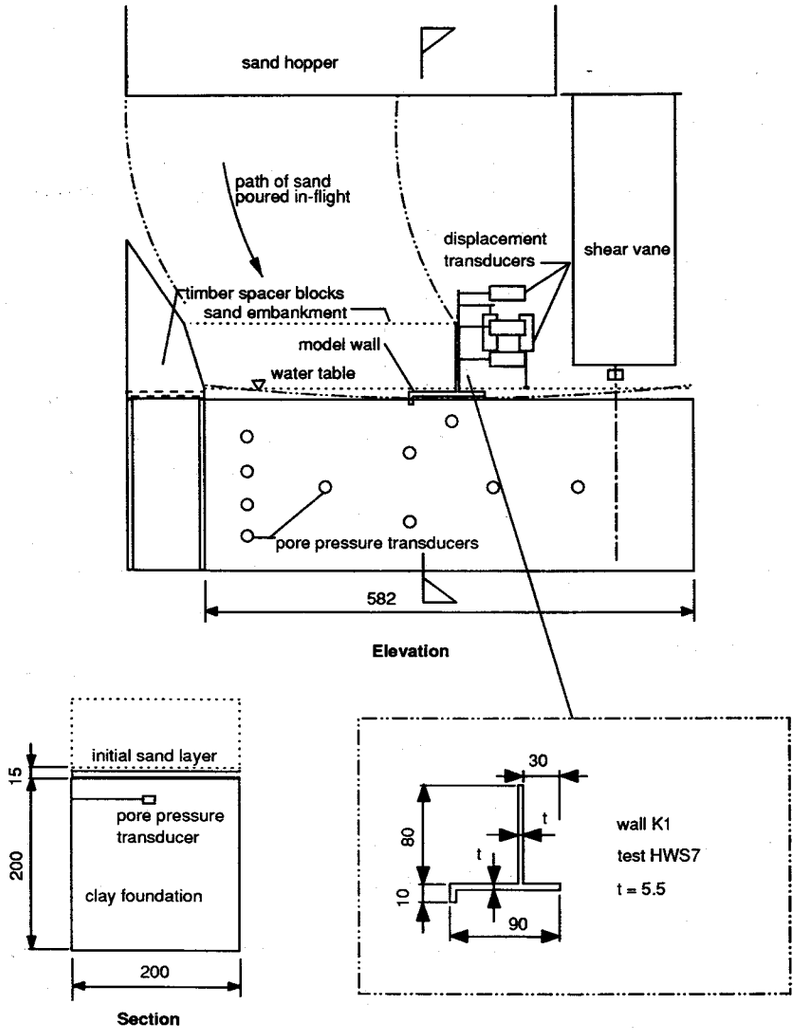

FIGURE 2. Typical arrangement of centrifuge model (test HWS7)

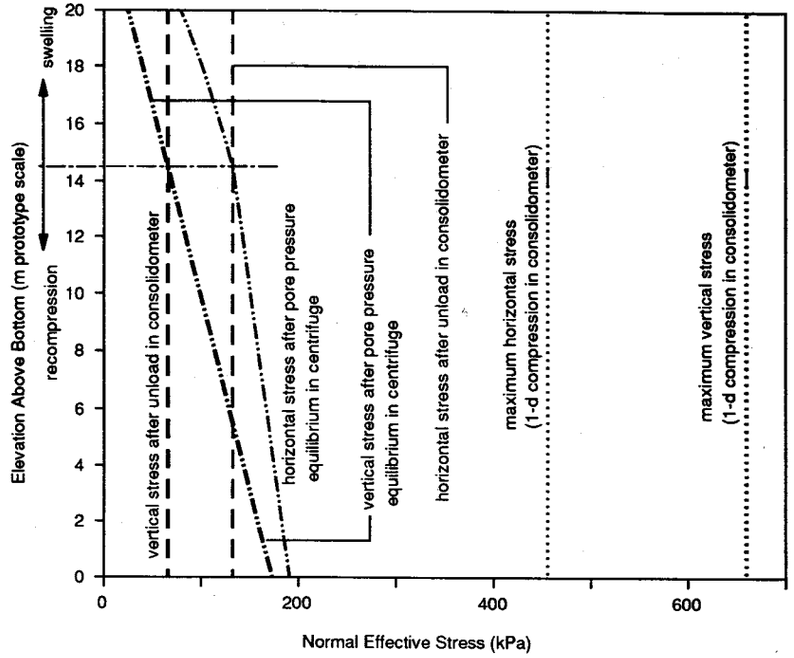

Figure 3. Stress state of clay foundation prior to embankment construction

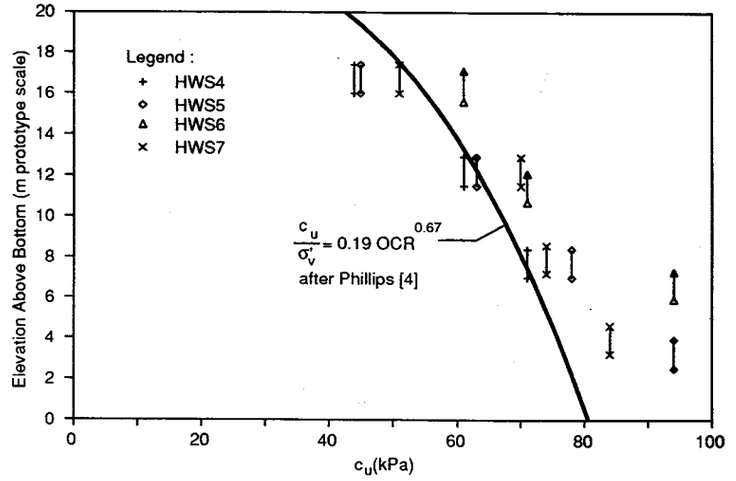

FIGURE 4. Undrained shear strength profile of the clay foundation measured by in-flight shear vane tests

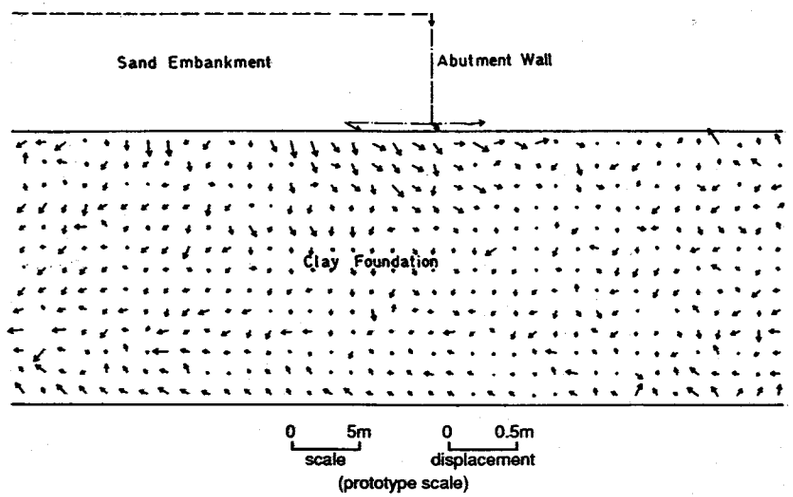

FIGURE 5. Subsoil displacement immediately after embankment construction - test HWS3

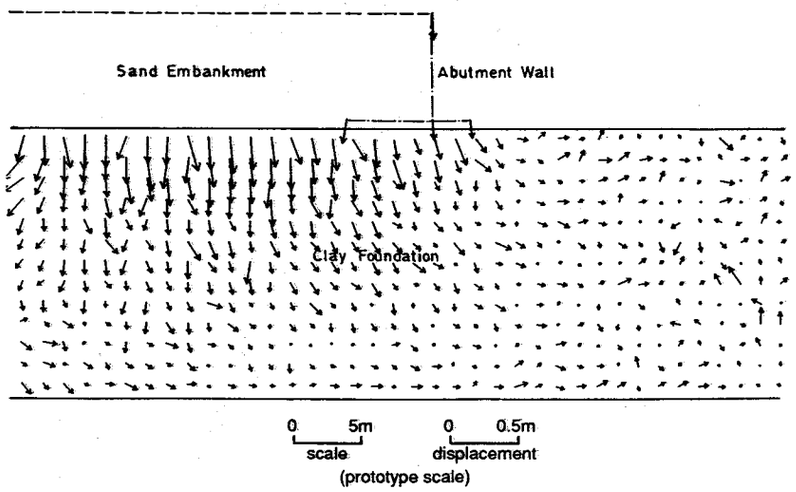

FIGURE 6. Subsoil displacement due to consolidation under embankment load - test HWS3

Consolidation of the model clay foundation took place in the next 5.5 to 6 hours (6 years and 3 months to 6 years and 10 months at prototype scale). Ground displacement due to consolidation was mainly one-dimensional settlement as observed from the in-flight photographs. Figure 6 shows the incremental subsoil displacement between undrained and consolidated states in test HWS3.

Differential settlement at the edge of the embankment caused the wall to move further forward and to rotate backwards, which also increased the lateral earth pressure acting behind the abutment wall. This was shown by a significant increase of the bending moments in the wall stem. Sun [3] describes the centrifuge tests in more detail.

THE STRESS-STRAIN RESPONSE OF THE CLAY FOUNDATION

The stress-strain response of an overconsolidated clay, which remains within the yield surface defined by its maximum consolidation pressure, is not linearly elastic. Non-linearity and anisotropy of the soil depend on the inherent anisotropy of its particle structure and the induced anisotropy of its current stress-path direction, stress and strain history.

Active and passive undrained cyclic stress path tests on vertical and horizontal plane-strain samples, as described in Sun [3], show different stress-strain responses which reflects the strong inherent anisotropy in stiffness of the one-dimensionally consolidated kaolin (figure 7), where the change of mobilized shear strength Δc is defined in figure 8. Cyclic stress-strain response following an imposed reversal of loading is almost unaffected by unknown stress-strain history during the sampling and setting-up processes. It is then necessary to select an origin for strain depending on whether the construction process reverses the prior strain direction in the model, or not.

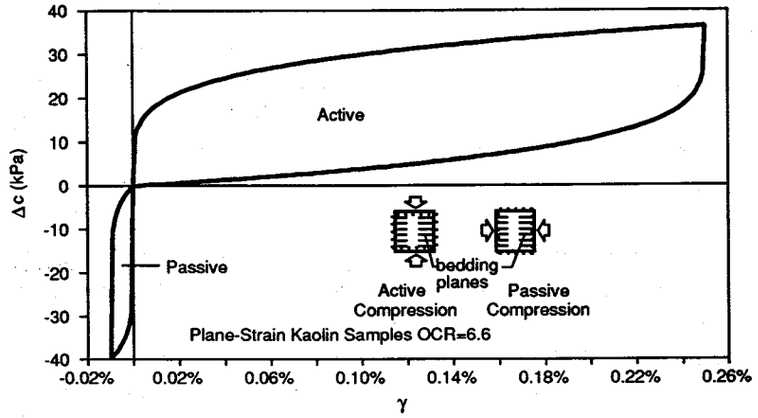

FIGURE 7. Undrained cyclic stress-strain response of overconsolidated kaolin

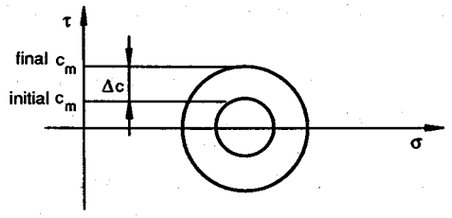

FIGURE 8. Mobilized shear strength of soil

Based on a stress and strain history analysis of the one-dimensional swelling and re-compression of the clay model (figure 9), the amount and directions of principal compressive strain in the clay model since the last strain reversal can be estimated. In one-dimensional deformation, volumetric strain is equal to shear strain (figure 10a). Despite the difference in strain path direction, this shear strain is taken to be equivalent to undrained shear strain in this analysis (figure 10b). Figure 11 shows the pre-strain profile in the clay model based on one-dimensional deformation from the last strain reversal. This pre-strain must be added to the newly imposed strain if that strain continues in the same direction. If the strain in the model reverses, the cyclic data of figure 7 can be applied directly without shifting the strain origin. The horizon at 5.45m depth initially separates shallow swelling soil from deeper consolidating soil. The strain

paths of soil at shallow (2m) and deep (8m) horizons (prototype scale) are shown on axes of shear strain ϵ_s against volumetric strain ϵ_v in figure 12. Figure 13 shows the expected undrained stress-strain response of the model clay elements at different depths. The potential significance of high stiffness after strain reversal is clear. Note in figure 13 that the element representing 2m depth, which had most recently been swelling, shows high stiffness in active loading, while that from the element representing 8m depth, which had most recently been consolidating, shows the opposite. Note also that there is little anisotropy of strength for samples tested in active and passive modes. The apparently different asymptotes of such tests in Figure 12 is due to the bias in initial shear stress: only changes Δc are plotted.

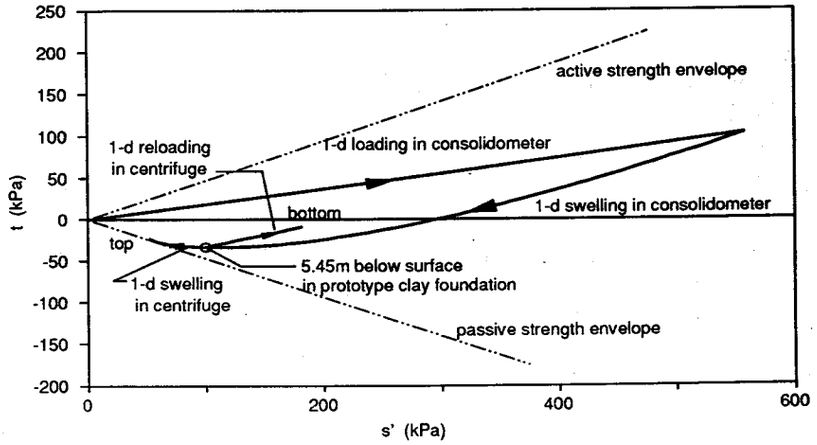

FIGURE 9. Stress history of centrifuge clay model

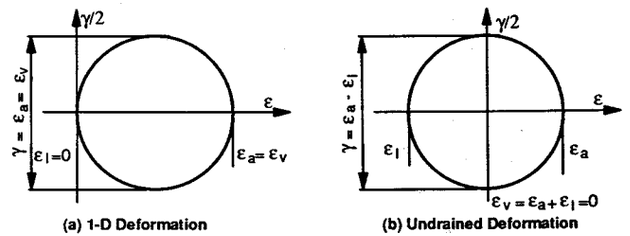

FIGURE 10. Mohr's circles of strain

Anisotropy leading to the predominance of vertical strain was also observed in the consolidation phase of clay specimens which had previously been subjected undrained to either vertical or horizontal major stress changes in the plane strain element tests. This helps to explain the dominance of vertical displacement in the consolidation of the clay foundation (figure 6).

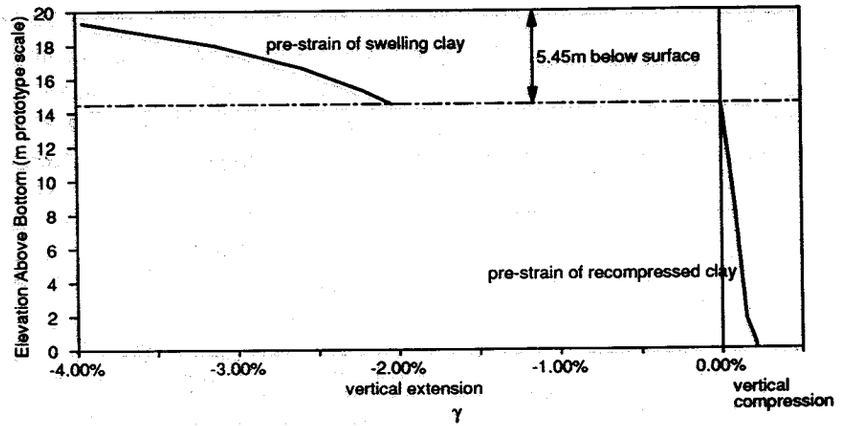

FIGURE 11. Pre-strain in the clay foundation prior to embankment construction

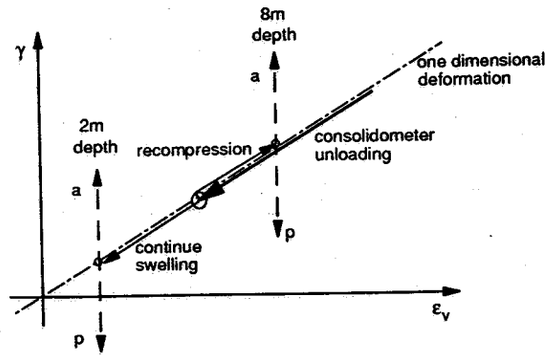

FIGURE 12. Strain plots of soil elements at depths of 2m and 8m (prototype scale) in active (a) and passive (p) zones

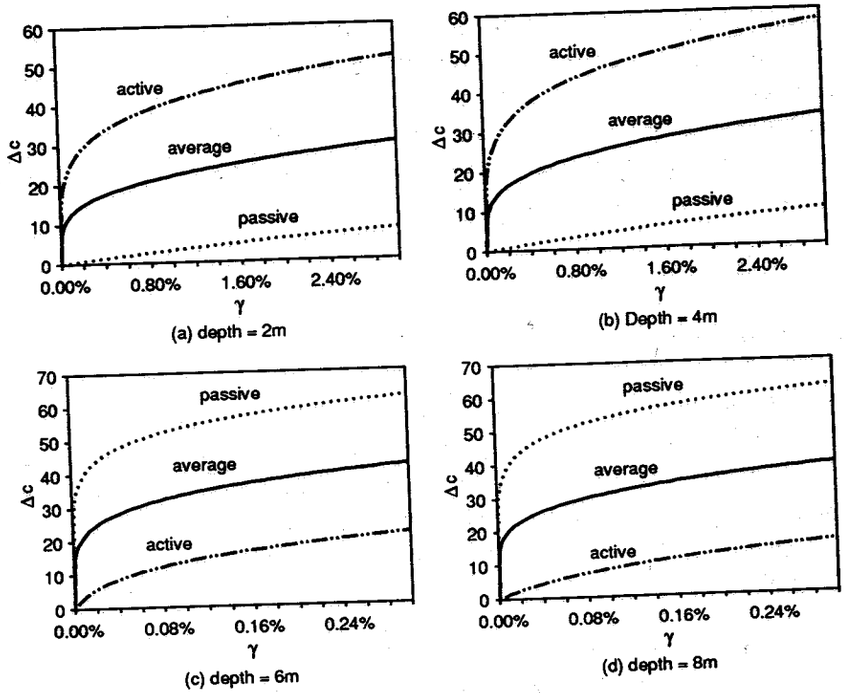

FIGURE 13. Stress-strain responses of clay elements

THE FINITE ELEMENT ANALYSES

The analyses were carried out for an idealized 100g centrifuge model at a prototype scale similar to test HWS7, but with a minor change in the abutment wall design (figure 2). The shear key in the model wall K1 of test HWS7 did not influence unduly the interaction between the wall base and its clay foundation compared with a flat base wall, since the movement was dominated by the subsoil displacement and not local sliding between the wall base and its clay foundation.

A modified version of the geotechnical finite element package CRISP90DP (double precision version of CRISP90) mounted on the IBM3084 computer of Cambridge University was used in this series of analyses. CRISP90 is specified in the user manual (Britto and

Gunn [5]), and the modification to implement a non-linear elastic soil model is described in Sun [3]. Output from the analyses was transferred to an IBM PC computer for presentation using a spreadsheet program, in addition to post-processing with the FEMVIEW program on the HP teaching workstations in the Cambridge University Engineering Department.

(a) The Geometry

Figure 14 shows the finite element mesh adopted for the analyses, which were conducted in plane-strain with similar boundary conditions to the centrifuge models. There are 94 linear strain triangle elements with displacement and pore pressure unknowns to simulate a 20m thick prototype foundation overlying a hard stratum. 22 linear strain quadrilateral elements are used to represent the initial sand layer on top of the clay foundation. 33 linear strain quadrilateral elements are employed to model the sand embankment which will be added in-place during the finite element analyses to simulate the construction of the embankment behind the abutment wall. The wall is represented by 9 beam elements, with 10 slip elements to model the interaction between the smooth wall surface and the initial sand layer or backfill. 17 slip elements, which are assigned the same material properties as the adjacent soil elements lie beneath the sand embankment and provide the necessary continuations of the soil-wall interface slip elements.

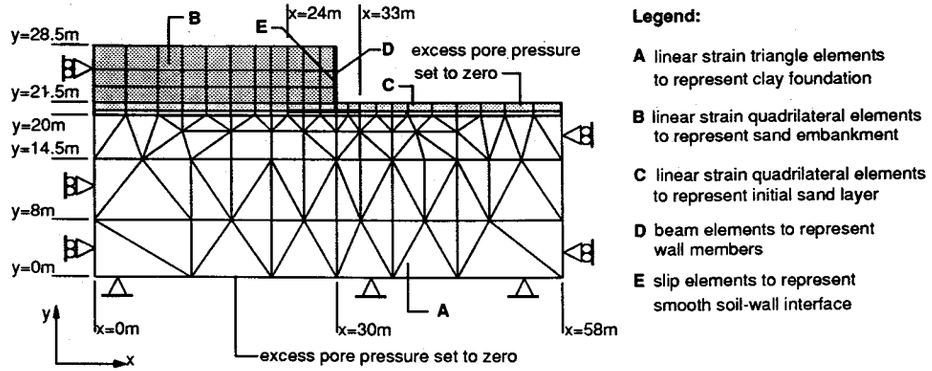

FIGURE 14. The finite element mesh

In the analyses, vertical boundaries of the foundation soil and the sand layers are allowed to slide and the bottom of the foundation soil is fixed in all directions. The top and bottom boundaries of the foundation soil are also assigned zero excess pore pressures to simulate the effect of the bottom and top drainage / water supplies in the centrifuge models.

(b) Material Modelling

The modelling of the soil behaviour of the foundation soil is very important in the analysis. A general soil model which is able to describe the stress-strain response of the foundation soil at different depths, as seen in figure 13, has not yet been implemented in CRISP: the difficulties are obvious.

Two more pragmatic schemes of calculation are now described. Considering the stress history and the undrained stress path expected in different areas of the foundation soil, it is divided into 6 zones arranged in 3 layers (figure 15). The 5.5m thick top layer represents the area of foundation clay which has been swelling (unloading) during the reconsolidation stage in the centrifuge. The clay deeper than 5.5m below the top surface has been re-compressed during the reconsolidation stage and is divided into two layers to allow different initial shear strain and confining pressures at different depths. The 3 zones immediately under the embankment are assumed to mobilize active stress paths. The other 3 zones are assumed to mobilize passive stress paths.

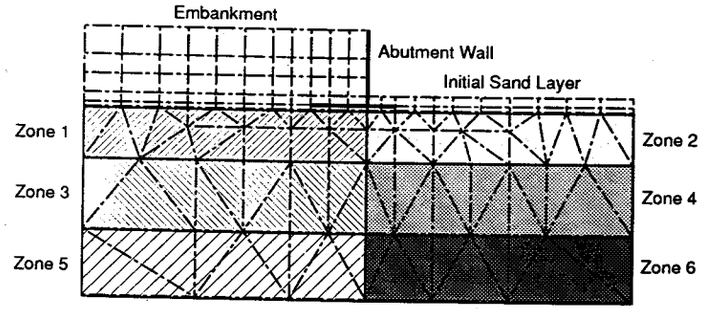

FIGURE 15. Idealized zones in the clay foundation

Scheme 1 uses a non-linear isotropic elastic model for the clay foundation based on a power-law for the shear stress-strain curve. Given an amount γ_i of pre-strain since the last strain reversal, the stress-strain relation for a further shear strain γ:

$$\tau = a(\gamma+\gamma_i)^b \quad \ldots\ldots\ldots \quad (1)$$

implies a tangent modulus

$$G = \frac{d\tau}{d\gamma} = ab(\gamma+\gamma_i)^{b-1} \quad \ldots\ldots\ldots \quad (2)$$

Based on the stress history and stress path analyses, Figure 16 shows the expected stress-strain responses in the 6 zones for finite element analysis with comments on behaviour due to its stress path and stress-strain history. Using this scheme, the analysis is carried out to model the undrained embankment construction only. The stress-strain response of foundation soil in the consolidation phase is not considered.

Scheme 2 uses the Schofield model with shear modulus G assigned to the foundation zone in accordance with the estimated strain level, stress history and stress path. Figure 16 shows the expected elastic shear stress-strain response of different foundation zones. As shown in figure 17, the Schofield model implemented in CRISP has the Hvorslev surface as an alternative yield locus on the dry side of the critical state and a Cam-Clay type yield surface on the wet side of critical state to define the yield surface of a soil (Schofield [6]). Normality of strain increments is imposed on every segment of the yield surface. Bolton et al [7] used the Schofield model in CRISP to analyse the collapse deformation of a diaphragm wall in heavily overconsolidated kaolin. The abutment wall in this problem is far from failure but, in the case of any local yielding, the use of the Schofield model will limit the shear strength of the overconsolidated clay compared with a Cam-Clay type yield surface on the dry side of the critical state. The critical state framework of the Schofield model in the consolidation analyses also enables

the analyses to be carried out into the consolidation phase after embankment building.

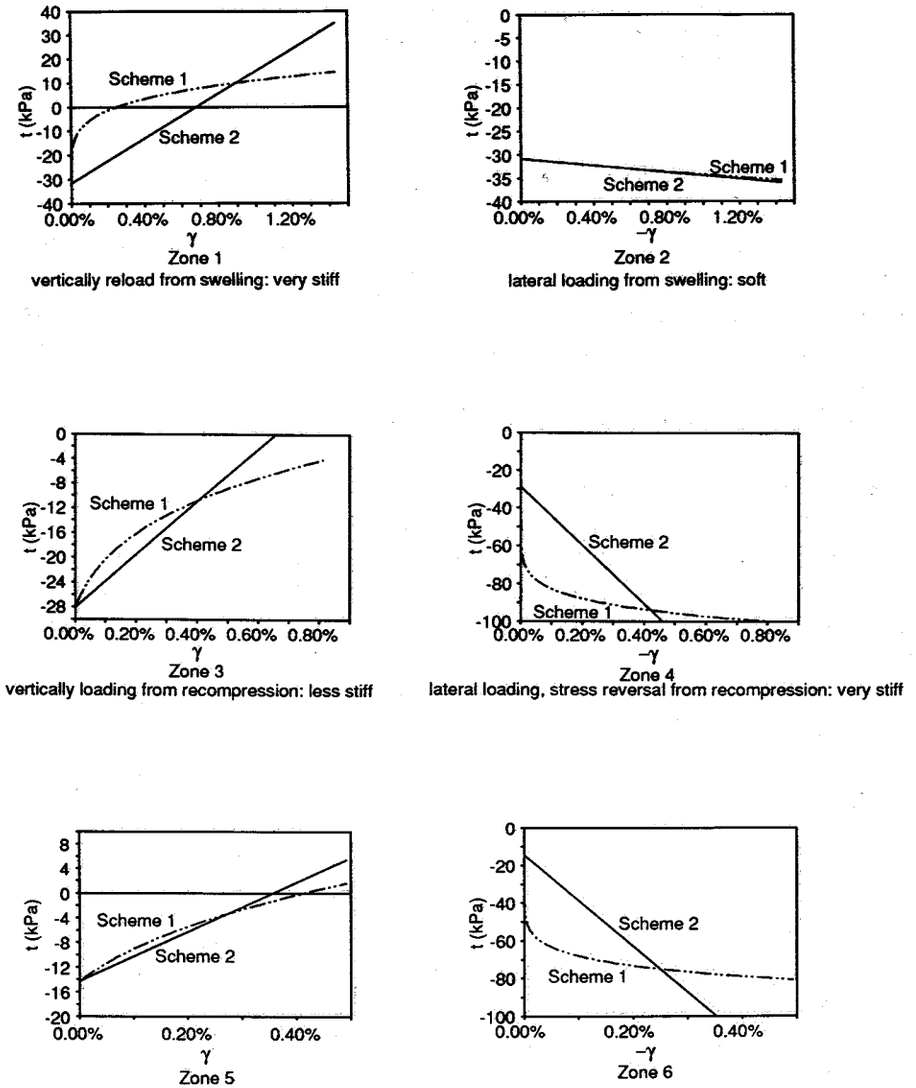

FIGURE 16. Expected elastic stress-strain response of clay foundation in finite element analyses schemes 1 and 2

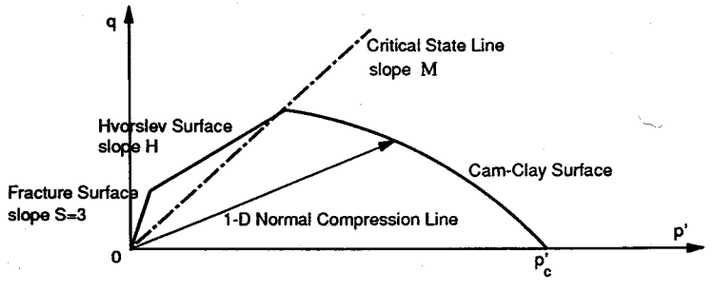

FIGURE 17. The yield surface of Schofield model

The critical state parameters adopted in the analysis scheme 2 are: M=0.9, Γ=3.44, λ=0.189 and κ=0.028 based on Al-Tabbaa [2]. The slope of the Hvorslev surface is taken to be H=0.59. The size of the initial yield surface is specified by the value of p'_c, figure 17. From the Cam-Clay yield surface and K_{onc}=0.69 with σ'_{vmax}=660kPa, p'_c is found to be 808kPa for the kaolin clay foundation.

An elastic perfectly plastic soil model is used to represent both the sand embankment and the initial sand layer in the finite element analyses. The shear strength parameters are ϕ=35° and c'=0 for the Mohr-Coulomb yield surface, and the elastic stiffness is specified in figure 18 for the dense embankment and the looser initial sand layer.

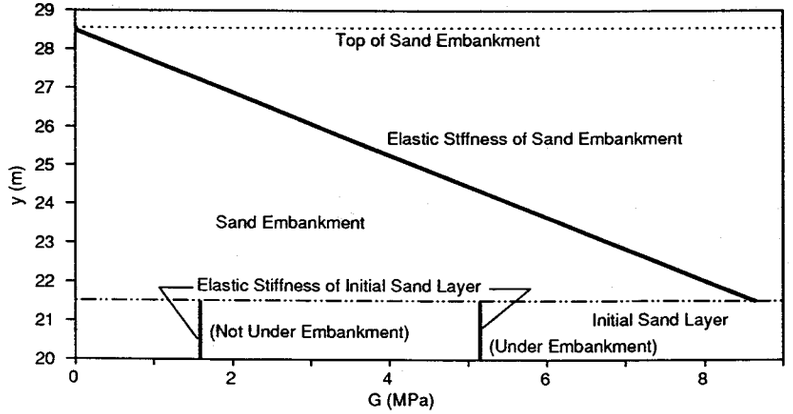

FIGURE 18. Elastic shear stiffness of sand embankment and initial sand layer in the finite element analyses

The wall members are modelled by beam elements in the analyses. Bending stiffness at prototype scale of the 5.5mm thick aluminium alloy model wall at 100g is modelled by E = 6.9 x 10^7 kN/m^2 and I = 0.01386 m^4/m compared with a 1m thick reinforced concrete member which has a similar long-term EI value.

With the exception of the bottom of the model wall base, the surfaces of the model wall are smooth and are modelled by a layer of slip elements. The slip element is assigned a stiffness similar to the adjacent soil elements and the yielding is controlled by Mohr-Coulomb strength parameters, c'=0 ϕ=15°, to model the maximum friction angle of the sand-wall interface. The thickness of the slip element is taken to be 0.001m.

The bottom of the wall base is assumed to be completely rough, the 0.5m thick linear strain quadrilateral elements are assigned identical material properties to those of the initial sand layer. Similarly, the slip elements which extended into the sand without attaching to a wall member (and which are required for geometrical reasons) are assigned material properties similar to those of the adjacent initial sand layer.

(c) The Analyses

The analyses were carried out in 3 stages (4 stages for scheme 2) using the CRISP stop-restart options with two magnetic tapes. The first 3 stages are to simulate the construction of an idealized embankment in level stages, by building up layers of elements behind the abutment wall (figure 19). Each stage is applied over 50 increments. Small load increments are adopted to prevent any numerical difficulties with the non-linear stress-strain responses of the soil elements. Stiffness of the sand elements are increased according to the height of the embankment.

The total time for the first 3 stages is 0.009 days to simulate the effects of undrained construction. Although the time step is much shorter than that in the centrifuge model tests (21 - 31 days at

prototype scale), the aim of the finite element analyses is to investigate an idealized case while matching approximately the centrifuge model. Similarly, the drifting of sand against the retaining wall, during the embankment construction by sand-pouring in the centrifuge model, is not considered; the process is idealized as placing of sand in layers of uniform thickness.

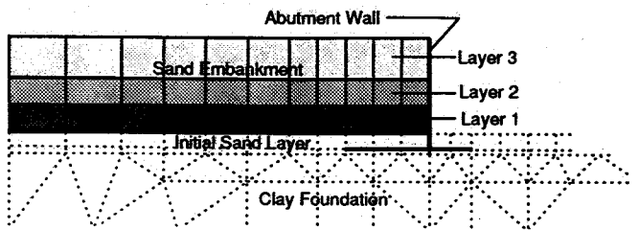

FIGURE 19. Staged building of elements to simulate embankment construction in finite element analyses

The consolidation phase of the analysis using scheme 2 was carried out in 140 increments over a time of 4 years and 11 months for the dissipation of excess pore pressure generated by the building of the embankment.

(d) The Results

The results of the finite element analyses of schemes 1 and 2 are to be compared with the results of centrifuge model test HWS7.

Immediately after the embankment construction, for an undrained condition of the clay foundation, the abutment wall moves forward causing the lateral pressure on the wall stem to drop to its active K value of 0.27 approximately (mobilizing ϕ=35°) in both analyses (figure 20). Amounts of wall movement from the two schemes in the finite element analyses and the centrifuge model test results are compared in figure 21.

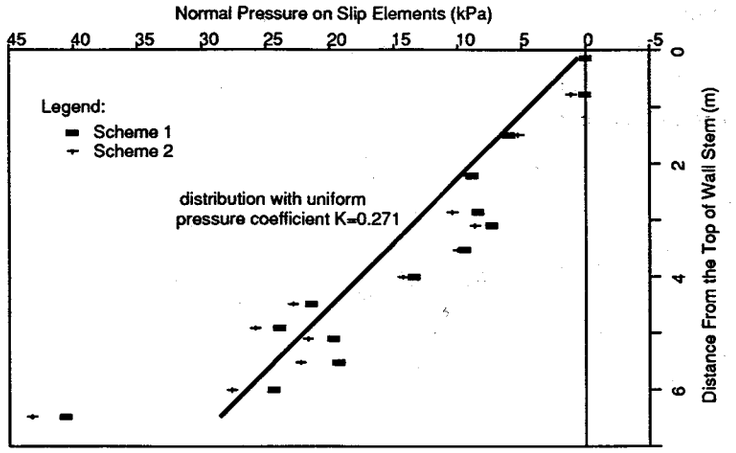

FIGURE 20. Lateral pressure on wall stem from finite element analyses

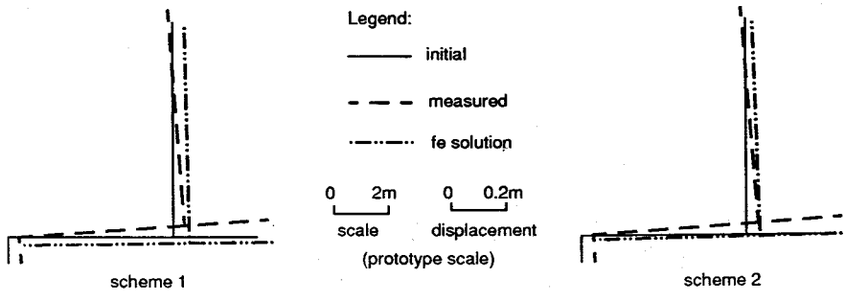

FIGURE 21. Predicted and measured wall movements for undrained foundation response - test HWS7

Predictions of horizontal wall movement at the base level agree approximately with the centrifuge model test result, but both schemes fail to estimate accurately the smaller vertical and larger rotational components of wall displacement.

To compare the ground displacement fields, figures 22 and 23 show the ground displacement vector plots determined from the finite element analyses. The ground displacements of analysis scheme 1 are concentrated near the edge of the embankment similar to those found from the subsoil movement in test HWS3 (figure 5). The ground

displacement distribution of scheme 2 is similar to that of scheme 1 but predicts slightly more widespread ground deformation. This may be due to the use of constant elastic modulus irrespective of the degree of deformation.

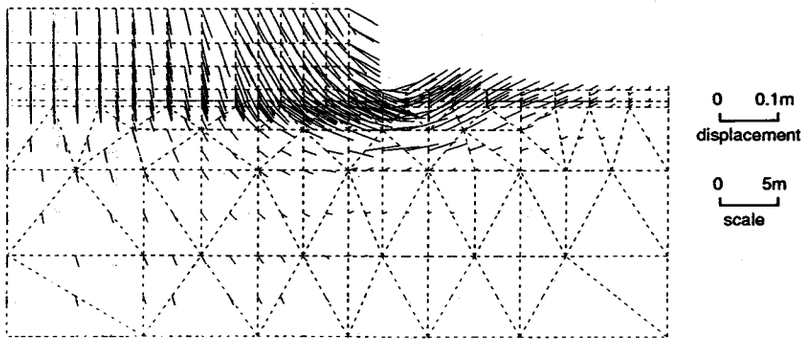

FIGURE 22. Ground displacement immediately after embankment construction - fe analysis scheme 1

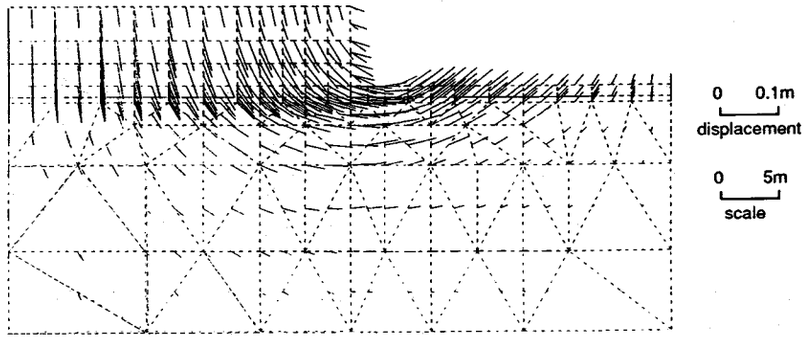

FIGURE 23. Ground displacement immediately after embankment construction - fe analysis scheme 2

The consolidation of the clay foundation causes differential settlement of the abutment wall at the edge of the embankment. Differential base settlement causes the wall to rotate backwards and leads to higher lateral pressure in the backfill. To model this interaction, the finite element analyses should first be able to

predict the ground displacements correctly. Figure 24 compares the settlement profile predicted by finite element analyses using scheme 2 and the result of centrifuge test HWS3 from the in-flight photographs. The finite element method underestimates the amount of settlement. This error may be due to the assumptions made in obtaining the κ value for the clay foundation. Figure 25 shows the ground displacement vectors during the consolidation phase as predicted in analysis scheme 2, which may be compared with the predominant vertical displacement observed in the model test and shown in figure 6. It also predicts backward movement of 0.023m at the wall base level, while continuous outward movement and backward rotation of the wall reference point were observed in centrifuge tests (figure 6). Figure 26 shows the final wall movement predictions and centrifuge test result.

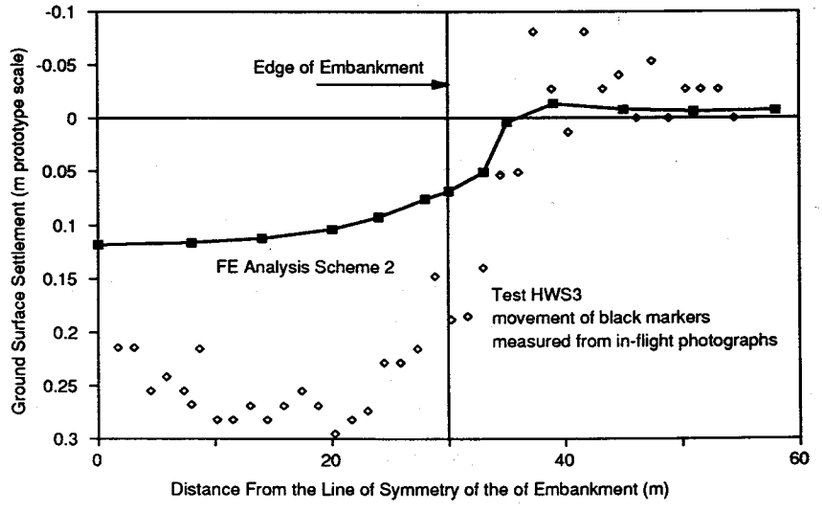

FIGURE 24. Final Settlement profile after the consolidation of clay foundation under embankment load

The prediction of final vertical wall movement agrees with the centrifuge model test results. However, the analysis fails to model the horizontal and rotational components of the wall movement during the consolidation stage. This may be due to modelling the consolidation deformation of an overconsolidated clay using a constant isotropic elastic modulus.

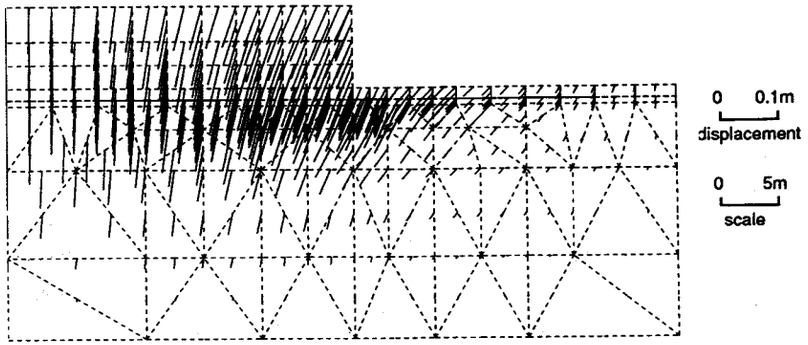

FIGURE 25. Vectors of subsoil displacement increment due to consolidation under embankment load - fe analysis scheme 2

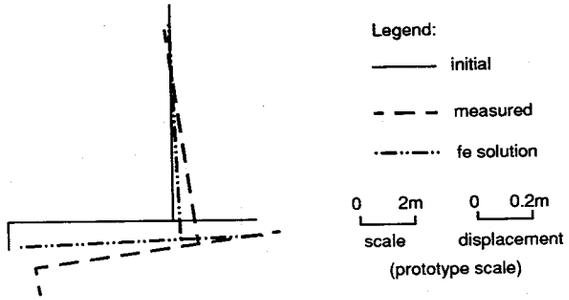

FIGURE 26. Predicted and measured wall movements after subsoil consolidation - test HWS7

CONCLUDING REMARKS

Soil models in finite element programs such as CRISP, which attempt to describe general soil behaviour with a minimum of parameters, can prove a robust tool in predicting modes of ground deformation. If the magnitudes of soil and structure displacements are required under working conditions, the values of soil parameters will have to be selected zone by zone to respect past and future strain paths. Some success is reported here on the prediction of the major

displacement components of an abutment wall on a spread base (horizontal displacement due to undrained shearing, vertical settlement due to consolidation) using data of relatively straightforward compression and extension tests together with 1-D consolidation tests. Difficulties were encountered with the overprediction of horizontal ground displacement due to consolidation, when using an isotropic elastic formulation within the Cam-Clay yield surface in the CRISP. Overconsolidated clay is highly anisotropic and consolidation displacement is predominantly vertical.

Finite element programs which feature a constitutive model incorporating hysteresis and plastic yielding, and which reflect inherent and strain-path-induced anisotropy in clay, are under development (Al-Tabbaa [2] and Stallebrass [8]). Although such models would go well beyond the "curve-fitting" approach to stress-path data which has been used in the present study, they would presumably require at least as much specialist soil testing. It remains to be seen whether such complex theoretical models can be developed and validated, against centrifuge model data, for example.

The use of finite element programs by non-specialists in design offices must be restricted to a comparison between similar structures constructed in similar ground conditions. Absolute predictions of soil-structure displacements must be based on a reflective assessment of soil parameters and guided by a comparative assessment of simplified mechanisms using hand calculations. This calls for expert judgement.

ACKNOWLEDGEMENTS

Wing Sun is grateful for the financial support of the Croucher Foundation of Hong Kong and the Overseas Research Student Award from the CVCP of British Universities for his PhD study at Cambridge University.

REFERENCES

1. U.S. Department of Transportation, (1985). Tolerable Movement Criteria for Highway Bridges. Final Report FHWA/RD-85/107, Federal Highway Administration, USA.

2. Al-Tabbaa, A., (1988). Permeability and Stress-Strain Response of Speswhite Kaolin, PhD Dissertation, Cambridge University, UK.

3. Sun, H.W., (1990). Ground Deformation Mechanisms for Soil-Structure Interaction, PhD Dissertation, Cambridge University, UK.

4. Phillips, R., (1988). Centrifuge Lateral Pile Tests in Clay, Tasks 2 & 3, a Report to Exxon Production Research Corp. by Lynxvale Ltd., Cambridge, UK.

5. Britto, A.M and Gunn, M.J., (1990). CRISP 90 User's and Programmers's Guide, Cambridge University, UK.

6. Schofield, A.N., (1980). Cambridge University Geotechnical Centrifuge Operations, Géotechnique, 30 (3), 1980, 227-268.

7. Bolton, M.D., Britto, A.M. and White, T.P. (1989). Finite Element Analyses of a Retaining Wall Embedded in a Heavily Overconsolidated Clay, Computers and Geotechnics, 7 (4), 289-318.

8. Stallebrass, S.E., (1990). Modelling Small Strains for Analysis in Geotechnical Engineering, Ground Engineering, 22, 26-29.

Received 18 February 1991; revised version received 8 April 1993; accepted 14 April 1993